Barcelona '10

A practical approach to compensate for the azimuth anisotropy in 3D PS converted wave processing

Hengchang Dai, and Xiang-Yang Li, British Geological Survey,
Chenye Yu, PetroChina Daqing Oilfield Limited
Jianmin Wang, CNPC Daqing Geophysical Exploration

A practical approach is developed to compensate for azimuthal anisotropy in 3D PS converted wave processing. This method involves fitting the measured velocity variation into a velocity ellipse and applying NMO correction with this velocity ellipse before stacking. We have derived a new least-square fitting algorithm and developed the necessary tools. The tools are applied to a land 3D dataset. The processing results show that the events with azimuthal variation in velocity applied are clearer and better focused, so that the image is enhanced.

Introduction

In recent years multi-component 3D seismic data have demonstrated their usefulness for characterising fractured reservoirs. Many theoretical and field studies have shown that azimuthal variation in attributes (such as velocity, amplitude) can be used as indicators of azimuthal anisotropy (Li *et al.*, 2003, Vetri *et al.*, 2003; and Zhu *et al.*, 2008, Qian *et al.*, 2008). Methods have been developed to extract the azimuthal anisotropy from PP and PS waves for inverting fracture properties. However, how to compensate for the effects of azimuthal anisotropy in imaging processing of 3D dataset is an unsolved problem. In this paper, we develop an approach to compensate for the azimuthal variation in 3D PS converted wave data processing. This method involves fitting the measured velocity variation into a velocity ellipse and applying this velocity ellipse to NMO correction before stacking. A real 3D dataset is used to test this approach.

Azimuthal variation of PS wave velocity and the moveout

In 3D data processing, the azimuthal anisotropy can be observed in the common-offset-common-azimuth cube (Zhu, 2008). After NMO correction, the residual NMO anomalies vary with azimuthal direction. This variation is normally represented as a cosine function. The NMO is controlled by the velocity model which includes four parameters: V_{ps}, γ_0, γ_{eff}, and χ_{eff} for PS converted-waves (Li and Yuan, 2003). The azimuthal variation in any of the four parameters may contribute to the azimuthal variation in residual NMO anomalies. However the four parameters have different sensitivities to PS wave moveout. The PS wave velocity V_{ps} is most sensitive. For weak anisotropy, the azimuthal variation in γ_0, γ_{eff}, and χ_{eff} can be neglected and only the azimuthal variation in V_{ps} considered. According to the azimuthal variation of residual NMO anomalies, the azimuthal variation in PS wave velocity can be written as:

$$V_{ps}(\theta) = V_0 + \alpha \cos 2(\theta - \beta)\,; \qquad (1)$$

where V_0 is the base velocity, α the velocity perturbation, and β the direction of the maximum velocity (e.g. the fracture direction), and θ the ray path azimuth. The PS converted wave moveout can then be written as:

$$t_{ps}^2 = t_{ps0}^2 + \frac{h^2}{V_{ps}^2(\theta)} - \frac{2\kappa_{eff} h^4}{V_{ps}^2(\theta)[t_0^2 V_{ps}^2(\theta) + m \cdot h^2]}. \qquad (2)$$

This moveout is used to perform the NMO correction in 3D PS converted wave data processing.

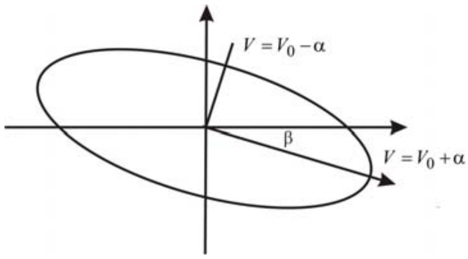

Figure 1 Ellipse of PS wave velocity which indicates the azimuthal variation of PS wave velocity in azimuthal anisotropic media.

Estimation of the azimuthal variation of PS-wave velocity

In order to use Equations (1) and (2) in 3D PS converted wave processing, we need to determine, V_0, α, and β. Although, the azimuthal anisotropy can be observed from the residual NMO in the common-offset-common-azimuth cube, it is difficult to directly quantify them from the residual NMO anomalies. One practical approach is to separate the 3D data into sections according to azimuth (Figure 2). For each section, we can assume that the data have the same anisotropy for the directions in the section data, so that conventional velocity analysis method and tools can be used. Once the velocity models for all sections are measured, we can fit the measured velocity into Equation (1).

Ellipse fitting

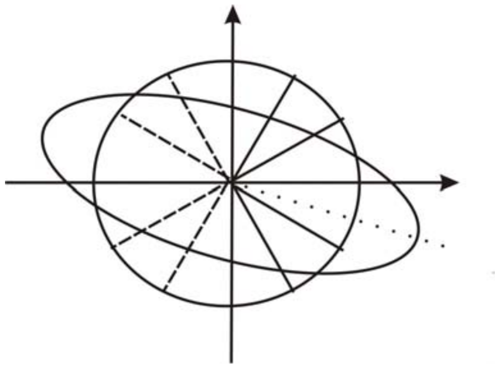

Figure 2. Seismic data is separated into sections according to azimuth. As the data is symmetrical with azimuth, all data section are combined into section between 0^o and 180^o.

To fit the measured velocity into Equation (1), an ellipse fitting method is necessary. A fair amount of research work has been accomplished in literature on ellipse fitting. Normally, the existing method of ellipse flitting is used for the ellipse represented by

$$Ax^2 + Bxy + Cy^2 + Dx + Ey + F = 0 \tag{3}$$

The best known method for fitting measured data to the ellipse is least-square fitting. Least-square fitting focuses on finding a set of parameters that minimize some distance measured between the data points and the ellipse. Although this method is very accurate, it is overly sensitive to outlines, and may perform poorly in the presence of outliers (Rosin, 1999). In addition, because the velocity variation is represented by Equation (1), a least-square fitting algorithm for Equation (1) is not available. Here, we derive the formulas which can be used to fit Equation (1).

For each section data, we can obtain a pair of velocity and azimuth (V_i, θ_i) based on PS wave velocity analysis. In order to fit the pairs into Equation (1), we define the error function as:

$$e(V_0, \alpha, \beta) = \sum [V_i - V_0 - \alpha \cdot \cos 2(\theta_i - \beta)]^2 \, . \tag{3}$$

To find the minimal values of e, we take the partial differential and have:

$$\frac{\partial e}{\partial V_0} = 2\sum [V_i - V_0 - \alpha \cdot \cos 2(\theta_i - \beta)]^2 = 0 \, ; \tag{4a}$$

$$\frac{\partial e}{\partial \alpha} = -2\sum [V_i - V_0 - \alpha \cdot \cos 2(\theta_i - \beta)] \cos 2(\theta_i - \beta) = 0 \, ; \tag{4b}$$

$$\frac{\partial e}{\partial \alpha} = -2\sum [V_i - V_0 - \alpha \cdot \cos 2(\theta_i - \beta)] \cos 2(\theta_i - \beta) = 0 \, ; \tag{4c}$$

The resolutions obtained from above equations are:

$$\tan 2\beta == \frac{\begin{array}{l} n\sum V_i \cos 2\theta_i \sum \cos 2\theta_i \sin 2\theta_i - n\sum (\cos 2\theta_i)^2 \sum V_i \sin 2\theta_i \\ + \sum V_i \sin 2\theta_i (\sum \cos 2\theta_i)^2 - \sum V_i \cos 2\theta_i \sum \cos 2\theta_i \sum \sin 2\theta_i \\ + \sum V_i \sum (\cos 2\theta_i)^2 \sum \sin 2\theta_i - \sum V_i \sum \cos 2\theta_i \sin 2\theta_i \sum \cos 2\theta_i \end{array}}{\begin{array}{l} n\sum V_i \sin 2\theta_i \sum \cos 2\theta_i \sin 2\theta_i - n\sum V_i \cos 2\theta_i \sum (\sin 2\theta_i)^2 \\ + \sum V_i \cos 2\theta_i (\sum \sin 2\theta_i)^2 - \sum V_i \sin 2\theta_i \sum \cos 2\theta_i \sum \sin 2\theta_i \\ + \sum V_i \sum (\sin 2\theta_i)^2 \sum \cos 2\theta_i - \sum V_i \sum \cos 2\theta_i \sin 2\theta_i \sum \sin 2\theta_i \end{array}} \, ; \tag{5}$$

$$\alpha = \frac{n\sum V_i \cos 2(\theta_i - \beta) - \sum V_i \sum \cos 2(\theta_i - \beta)}{n\sum [\cos 2(\theta_i - \beta)^2] - [\sum \cos 2(\theta_i - \beta)]^2} \, ; \tag{6}$$

and

$$V_0 = \frac{\sum V_i - \alpha \sum \cos 2(\theta_i - \beta)}{n} \, ; \tag{7}$$

Once β, α, and V_0 are determined, Equation (1) is used in the NMO correction. For each trace, the azimuthal direction is calculated based on the source and receiver locations. The velocity and the moveout for the azimuthal direction are calculated for NMO correction.

Data example

Figure 3 shows the processing flow to compensate for the azimuth anisotropy. The difference between our approach and the conventional one is that we apply the ellipse velocity in the NMO before stacking. The azimuthal anisotropy is compensated for in the NMO correction.

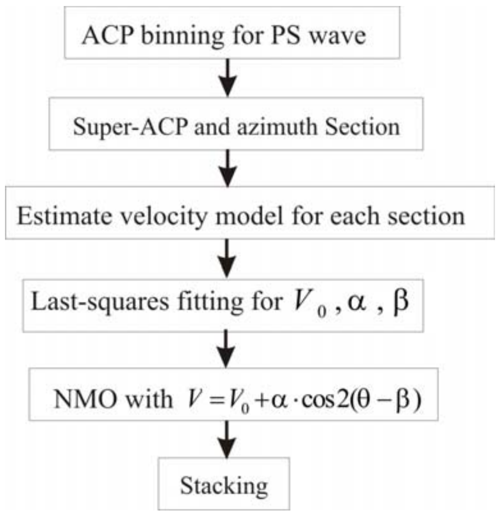

Figure 3. Processing flow for compensating

This processing flow is applied to two swath data of a land 3D dataset acquired in Daqing oil field. Figure 4 shows the geometry of the dataset. Only data with short and middle offsets have full azimuthal coverage. The ACP binning is applied to the dataset and super ACP gathers are formed by combining 20 adjacent CDP gathers in 20 adjacent CDP-lines (20x20). The Super-gather is then separated into six sections with azimuthal widths of 30º. For each section data, the PS converted wave velocity analysis is applied to measure the PS wave velocity. Note γ_0, γ_{eff}, and χ_{eff} are not various for all azimuthal section data. Figure 5 shows an example of the measured velocities and ellipse fitting result at time 1.47 second for one super-CDP gather. The azimuthal variation of the PS converted wave velocity can be written as:

$$V = 1282 + 74\cos 2(\theta - 30^0) \quad \textbf{(8)}$$

This velocity is applied to the NMO correction before stacking. Figure 6 is an example which shows the comparison between the NMO corrected super-gather with and without applied the azimuthal variation. The azimuthal variation is only observed for events between 1.3 second and 1.6 second (see rectangle in Figure 6). For the deep events, we cannot observer the azimuthal variation in as the data at far offset may not have enough azimuthal coverage or the azimuthal anisotropy may not exist. The events with azimuthal variation velocity applied (Figure 6b) are clearer and better focused than in Figure 6a. However, as the velocity perturbation is small (74/s/1282=5.8%), the improvement is not very significant. Note that the accuracy of β depends on the azimuthal width of the section. In order to increase the accuracy of β, the azimuthal width of the section data have to be reduced. However, the numbers of traces in data section are also reduced, and may mean that there are not enough data for velocity analysis.

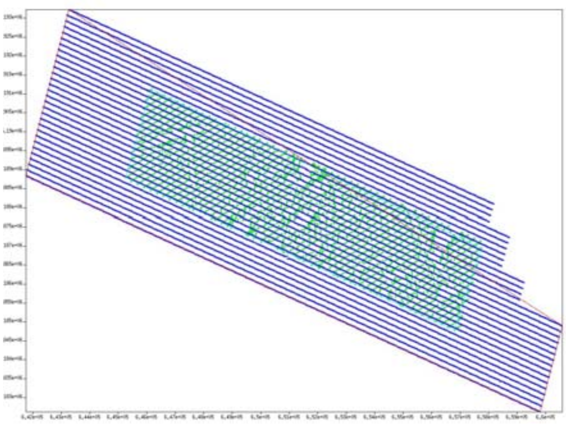

Figure 4. The geometry of two swath data of the land 3D datasets.

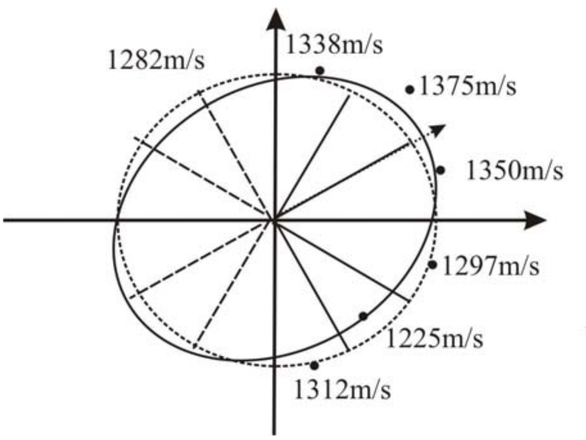

Figure 5. Example of measured PS wave velocity and ellipse fitting results.

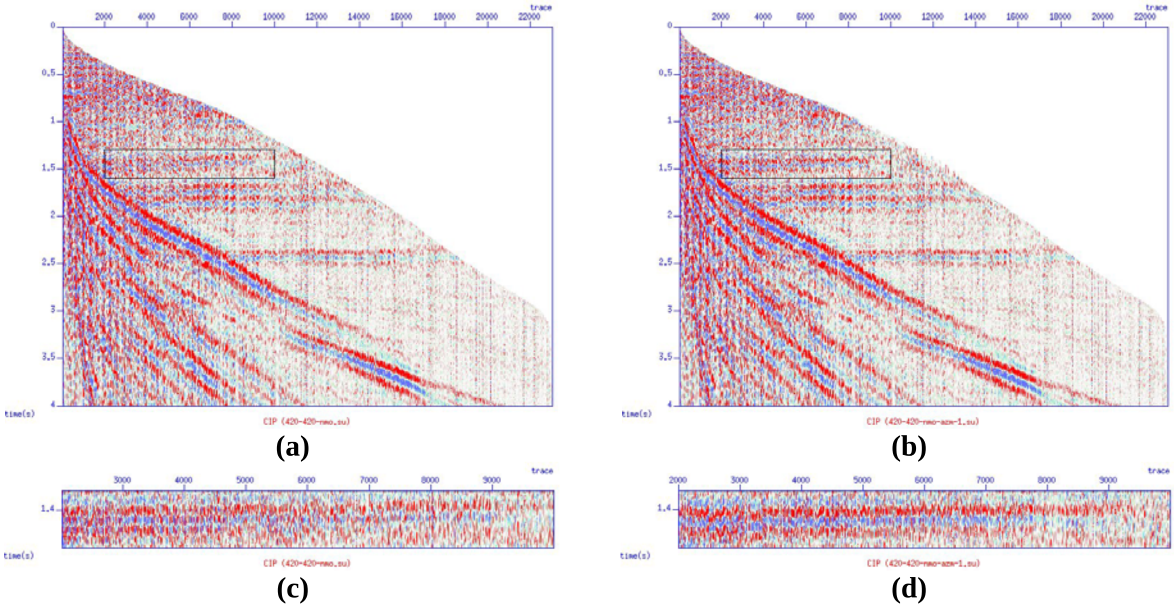

Figure 6. (a) Residual NMO without azimuthal variation velocity in a super ACP gather. (b) Residual NMO with azimuthal variation velocity in the same ACP super-gather. (c) and (d) are enlarged picture of the rectangle in (a) and (b), respectively, and indicate the event which we measured its azimuthal anisotropy and applied the velocity with and without azimuthal variation.

Summary

In this work, we propose an approach to compensate for the azimuthal anisotropy in 3D PS converted-wave data processing. The key steps in this approach are to obtain the velocity ellipse by measuring the velocity in section data and fitting the measured velocity into the velocity ellipse, and then apply the velocity ellipse to NMO corrections before stacking. We have derived a new least-square fitting algorithm and developed the necessary tools. The tools are applied to a land 3D dataset. The processing results show that the events with azimuthal variation in velocity applied are clearer and better focused so that the image is enhanced. Further research should include how to decide azimuthal width and apply this to pre-stack time migration.

Acknowledgements

We thank Daqing Oil Field of China for providing the 3D datasets. This work is supported by the Edinburgh Anisotropy Project (EAP) of the British Geological Survey, and is published with the permission of the Executive Director of the British Geological Survey (NERC) and the EAP sponsors.

References

Li, X.-Y. and Yuan, J., 2003, Converted-wave moveout and conversion-point equations in layered VTI media: theory and applications, Journal of Applied Geophysics, **54**, 297-318.

Li, X., Liu, Y., Liu, E, Shen, F., Li, Q., Qu, S., 2003, Fracture detection using land 3D seismic data from the Yellow River data, China, The Leading Edge, July 2003, 680-683;

Rosin, P., 1999, Further five-point fit ellipse fitting, Graphical Models and Image Processing, **61,** 5, pp. 245-259, 1999.

Qian, Z., Li, X., and Chapman, M., 2008, Fracture characterization with azimuthal attribute analysis of PS-wave data: modelling and application, 70th EAGE Meeting, Expanded Abstracts, June 2008, Rome

Vetri, L., Loinger, E., Gaiser, J., Grandi, A., Lynn, H., 2003, 3D/4C Emilio Azimuth processing and anisotropy analysis in a fractured carbonate reservoir, The Leading Edge, July 2003, 675-679;

Zhu, X., Valasek, P., Roy, B., Shaw, S., Howell, J., Whitney, S., Whitmore, N., Anno, P., 2008, Recent application of turning ray tomography, Geophysics, **73**, 5, VE243-VE254